



A pan-African high-resolution drought index dataset

Jian Peng^{1,2}, Simon Dadson¹, Feyera Hirpa¹, Ellen Dyer¹, Thomas Lees¹, Diego G. Miralles³, Sergio M. Vicente-Serrano⁴, Chris Funk^{5,6}

1. School of Geography and the Environment, University of Oxford, OX1 3QY Oxford, UK;

2. Max Planck Institute for Meteorology, Hamburg, Germany;

3. Laboratory of Hydrology and Water Management, Ghent University, Ghent, Belgium;

4. Instituto Pirenaico de Ecología, Consejo Superior de Investigaciones Científicas (IPE-CSIC) Zaragoza, Spain;

5. U.S. Geological Survey, Earth Resources Observation and Science Center, Sioux Falls, South Dakota;

6. Santa Barbara Climate Hazards Center, University of California, USA;

Corresponding author: Jian Peng (jian.peng@ouce.ox.ac.uk)

Abstract

Droughts in Africa cause severe problems such as crop failure, food shortages, famine, epidemics and even mass migration. To minimize the effects of drought on water and food security over Africa, a high-resolution drought dataset is essential to establish robust drought hazard probabilities and to assess drought vulnerability considering a multi- and cross-sectorial perspective that includes crops, hydrological systems, rangeland, and environmental systems. Such assessments are essential for policy makers, their advisors, and other stakeholders to respond to the pressing humanitarian issues caused by these environmental hazards. In this study, a high spatial resolution Standardized Precipitation-Evapotranspiration Index (SPEI) drought dataset is presented to support these assessments. We compute historical SPEI data based on Climate Hazards group InfraRed Precipitation with Station data (CHIRPS) precipitation estimates and Global Land Evaporation Amsterdam Model (GLEAM) potential evaporation estimates. The high resolution SPEI dataset (SPEI-HR) presented here spans from 1981 to 2016 (36 years) with 5 km spatial resolution over the whole Africa. To facilitate the diagnosis of droughts of different durations, accumulation periods from 1 to 48 months are provided. The quality of the resulting dataset was compared with coarse-resolution SPEI based on Climatic Research Unit (CRU) Time-Series (TS) datasets, and Normalized Difference Vegetation Index (NDVI) calculated from the Global Inventory Monitoring and Modeling System (GIMMS) project, as well as with root zone soil moisture modelled by GLEAM. Agreement found between coarse resolution SPEI



30 from CRU TS (SPEI-CRU) and the developed SPEI-HR provides confidence in the estimation of temporal
31 and spatial variability of droughts in Africa with SPEI-HR. In addition, agreement of SPEI-HR versus NDVI
32 and root zone soil moisture – with average correlation coefficient (R) of 0.54 and 0.77, respectively – further
33 implies that SPEI-HR can provide valuable information to study drought-related processes and societal
34 impacts at sub-basin and district scales in Africa. The dataset is archived in Centre for Environmental Data
35 Analysis (CEDA) with link: <http://dx.doi.org/10.5285/bbdfd09a04304158b366777eba0d2aeb> (Peng et al.,
36 2019a)

37 **Keywords:**

38 Drought, Africa, Drought index, High resolution, Precipitation, Potential evaporation, drought management,
39 disaster risk reduction

40
41
42
43
44
45
46
47
48
49
50
51
52
53
54
55
56
57
58
59
60



61

62 **1 Introduction**

63 Drought is a complex phenomenon that affects natural environments and socioeconomic systems in the
64 world (Van Loon, 2015; Vicente-Serrano, 2007; von Hardenberg et al., 2001; Wilhite and Pulwarty, 2017).
65 Impacts include crop failure, food shortage, famine, epidemics and even mass migration (Ding et al., 2011;
66 Wilhite et al., 2007; Zhou et al., 2018). In recent years, severe events have occurred across the world, such as
67 the 2003 central Europe drought (García-Herrera et al., 2010), the 2010 Russian drought (Spinoni et al.,
68 2015), the 2011 Horn of Africa drought (Nicholson, 2014), the southeast Australian's Millennium drought
69 (van Dijk et al., 2013), the 2013/2014 California drought (Swain et al., 2014), the 2014 North China drought
70 (Wang and He, 2015) and the 2015–2017 Southern Africa drought (Baudoin et al., 2017; Muller, 2018).
71 Widespread negative effects of these droughts on natural and socioeconomic systems have been reported
72 afterwards (Arpe et al., 2012; Griffin and Anchukaitis, 2014; Mann and Gleick, 2015; Wegren, 2011). Thus,
73 there is a clear need to improve our knowledge about the spatial and temporal variability of drought, which
74 provides a basis for quantifying drought impacts and the exposure of society, the economy and the
75 environment over different areas and time-scales (AghaKouchak et al., 2015).

76 Generally, drought is defined as a temporal anomaly characterized by a deficit of water compared with long-
77 term conditions (Mishra and Singh, 2010; Van Loon, 2015). Droughts can typically be grouped into five
78 types: meteorological (precipitation deficiency), agricultural (soil moisture deficiency), hydrological (runoff,
79 groundwater deficiency), socioeconomic (social response to water supply and demand) and environmental or
80 ecologic (AghaKouchak et al., 2015; Crausbay et al., 2017; Keyantash and Dracup, 2002). These different
81 drought categories involve different event characteristics in terms of timing, intensity, duration, and spatial
82 extent, making it very difficult to characterize droughts quantitatively (Lloyd-Hughes, 2014; Panu and
83 Sharma, 2002; Vicente-Serrano, 2016). For this reason numerous drought indices have been proposed for
84 precise applications, and reviews of the available indices have been provided by previous studies such as
85 Heim Jr (2002), Keyantash and Dracup (2002), and Mukherjee et al. (2018). Van Loon (2015) noted that



86 there is no best drought index for all types of droughts, because every index is designed for a specific
87 drought type, thus multiple indices are required to capture the multifaceted nature of drought. Nevertheless,
88 the Standardized Precipitation Index (SPI) is recommended by the World Meteorological Organization
89 (WMO) for drought monitoring, which is calculated based solely on long-term precipitation data over
90 different time spans (McKee et al., 1993). The advantages of SPI are its relative simplicity and its ability to
91 characterize different types of droughts given the different times of response of different usable water
92 sources to precipitation deficits (Kumar et al., 2016; Zhao et al., 2017). However, information on
93 precipitation is not enough to characterize drought; in most definitions, drought conditions also depend on
94 the demand of water vapor from the atmosphere. More recently, Vicente-Serrano et al. (2010) proposed an
95 alternative drought index for SPI, which is called Standardized Precipitation Evapotranspiration Index
96 (SPEI). Compared to SPI, it considers not only the precipitation supply, but also the atmospheric evaporative
97 demand (Beguería et al., 2010; Vicente-Serrano et al., 2012b). This makes the index more informative of the
98 actual drought effects over various natural systems and socioeconomic sectors (Bachmair et al., 2016;
99 Bachmair et al., 2018; Kumar et al., 2016; Peña-Gallardo et al., 2018a; Peña-Gallardo et al., 2018b; Sun et
100 al., 2018; Sun et al., 2016c; Vicente-Serrano et al., 2012b).

101 For the calculation of SPEI, high-quality and long-term observations of precipitation and atmospheric
102 evaporative demand are necessary. These observations may either come from ground-based station data or
103 gridded data such as satellite and reanalysis datasets. For example, the SPEIbase (Beguería et al., 2010) and
104 the Global Precipitation Climatology Centre Drought Index (GPCC-DI) (Ziese et al., 2014) both provide
105 SPEI datasets at global scale. The SPEIbase provides gridded SPEI with a 50-km spatial resolution, and is
106 calculated from Climatic Research Unit (CRU) Time-Series (TS) datasets, which are produced based on
107 measurements from more than 4000 ground-based weather stations over the world (Harris et al., 2014). The
108 SPEI dataset provided by GPCC-DI has spatial resolution of 1°, and was generated from GPCC precipitation
109 (Becker et al., 2013; Schneider et al., 2016) and National Oceanic and Atmospheric Administration
110 (NOAA)'s Climate Prediction Center (CPC) temperature dataset (Fan and Van den Dool, 2008). Both of



111 these datasets have been applied for various drought related studies at global and regional scales (e.g., Chen
112 et al., 2013; Deo et al., 2017; Isbell et al., 2015; Sun et al., 2016a; Vicente-Serrano et al., 2016; Vicente-
113 Serrano et al., 2013). However, these global SPEI data sets' spatial resolution are too coarse to be applied at
114 district or sub-basin scales (Vicente-Serrano et al., 2017). A sub-basin scale quantification of drought
115 conditions is particularly crucial in regions such as Africa, in which geospatial data and drought indices can
116 be essential to manage existing drought-related risks (Vicente-Serrano et al., 2012a) and where in-situ
117 measurements are scarce (Anghileri et al.; Masih et al., 2014; Trambauer et al., 2013). Over last century,
118 Africa has been severely influenced by intense drought events, which has led to food shortages and famine
119 in many countries (Anderson et al., 2012; Awange et al., 2016; Funk et al., 2018; Sheffield et al., 2014;
120 Yuan et al., 2013). Therefore, the availability of a high-resolution drought index dataset may contribute to an
121 improved characterization of drought risk and vulnerability, and minimize its impact on water and food
122 security by supporting policy makers, water managers and stakeholders. Conveniently, with the
123 advancement of satellite technology, the estimation of precipitation and evaporation from remote sensing
124 datasets is becoming more accurate (Fisher et al., 2017). In particular, the long-term Climate Hazards group
125 InfraRed Precipitation with Station data (CHIRPS) (Funk et al., 2015a) precipitation and Global Land
126 Evaporation Amsterdam Model (GLEAM) (Miralles et al., 2011) evaporation datasets provide high-quality
127 datasets for near-real time drought monitoring. Here, we use CHIRPS and GLEAM datasets to develop a
128 pan-African high spatial resolution (5-km) SPEI dataset, which may be useful to inform drought relief
129 management strategies for the continent. The dataset covers the period from 1981 to 2016 and it is
130 comprehensively inter-compared with soil moisture, vegetation index and coarse resolution SPEI datasets.

131 **2 Data and Methodology**

132 2.1 Data

133 2.1.1 CHIRPS

134 CHIRPS is a recently-developed high-resolution, daily, pentadal, dekadal, and monthly precipitation dataset
135 (Funk et al., 2015a). It was produced by blending a set of satellite-only precipitation values (CHIRP) with



136 additional monthly and pentadal station observations. The CHIRP is based on infrared cold cloud duration
137 (CCD) estimates calibrated with the Tropical Rainfall Measuring Mission Multi-satellite Precipitation
138 Analysis version 7 (TMPA 3B42 v7) and the Climate Hazards group Precipitation climatology (CHPclim)
139 The CHP_{clim} (Funk et al., 2015a; Funk et al., 2015e) is based on station data from the Food and Agriculture
140 Organization (FAO) and the Global Historical Climate Network (GHCN). Compared with other global
141 precipitation datasets such as Multi-Source Weighted-Ensemble Precipitation (MSWEP) (Beck et al., 2017)
142 and Global Precipitation Climatology Project (GPCP) (Adler et al., 2003), CHIRPS has several advantages:
143 a long period of record, high spatial resolution (5-km), low spatial biases and low temporal latency. It has
144 been widely validated and applied in various applications (e.g., Duan et al., 2016; Maidment et al., 2015;
145 Rivera et al., 2018; Shukla et al., 2014; Zambrano-Bigiarini et al., 2017). In particular, it was recently
146 validated over East Africa and Mozambique and demonstrated good performance compared to other
147 precipitation datasets (Dinku et al., 2018; Toté et al., 2015). Furthermore, CHIRPS was specifically designed
148 for drought monitoring over regions with deep convective precipitation, scarce observation networks and
149 complex topography (Funk et al., 2014). Its high spatial resolution makes it particularly suitable for local-
150 scale studies, such as sub-basin drought monitoring, especially in areas with complex topography. The
151 detailed description of the dataset was provided by Funk et al. (2015a). In this study, daily CHIRPS
152 precipitation from 1981 to 2016 was used.

153 2.2.2 GLEAM

154 GLEAM is designed to estimate land surface evaporation and root-zone soil moisture from remote sensing
155 observations and reanalysis data (Martens et al., 2017; Miralles et al., 2011). Specifically, the Priestley-
156 Taylor equation is used to calculate potential evaporation within GLEAM based on near surface temperature
157 and net radiation, while the root zone soil moisture is obtained from a multilayer water balance driven by
158 precipitation observations and updated with microwave soil moisture estimates (Martens et al., 2017). The
159 actual evaporation is estimated by constraining potential evaporation with a multiplicative evaporative stress
160 factor based on root-zone soil moisture and Vegetation Optical Depth (VOD) estimates. The GLEAM



161 version 3a (v3a) provides global daily potential and actual evaporation, evaporative stress conditions and
162 root zone soil moisture from 1980 to 2018 at spatial resolution of 0.25° (Martens et al., 2017) (see
163 www.gleam.eu). GLEAM datasets have already been comprehensively evaluated against FLUXNET
164 observations and used for multiple hydro-meteorological applications (Forzieri et al., 2017; Greve et al.,
165 2014; Lian et al., 2018; Miralles et al., 2014; Richard et al., 2018; Vicente-Serrano et al., 2018). In particular,
166 two recent studies detected global drought conditions based on GLEAM potential and actual evaporation
167 data (Peng et al., 2019b; Vicente-Serrano et al., 2018). For this study, the GLEAM potential evaporation and
168 root zone soil moisture were used.

169 2.2.3 CRU-TS

170 The global gridded CRU-TS datasets provide most widely-used climate variables including precipitation,
171 potential evaporation, diurnal temperature range, maximum and minimum temperature, mean temperature,
172 frost day frequency, cloud cover and vapour pressure (Harris et al., 2014). The CRU TS datasets were
173 produced using angular-distance weighting (ADW) interpolation based on monthly meteorological
174 observations collected at ground-based stations across the world. The recently-released CRU TS version
175 4.0.1 covers the period 1901–2016 and provides monthly data at 50-km spatial resolution. The CRU TS
176 datasets have been widely used for various applications since their release (e.g., Chadwick et al., 2015;
177 Delworth et al., 2015; Jägermeyr et al., 2016; van der Schrier et al., 2013). The SPEIbase dataset was
178 generated from CRU TS datasets (Beguería et al., 2010). In this study, the CRU TS precipitation and
179 potential evaporation from 1981 to 2016 were used.

180 2.2.4 GIMMS NDVI

181 The Normalized Difference Vegetation Index (NDVI) can serve as a proxy of vegetation status and has been
182 widely applied to investigate the effects of drought on vegetation (e.g., Törnros and Menzel, 2014; Vicente-
183 Serrano et al., 2013; Vicente-Serrano et al., 2018). The Global Inventory Monitoring and Modeling System
184 (GIMMS) NDVI was generated based on Advanced Very High Resolution Radiometer (AVHRR)



185 observations, and has accounted for various deleterious effects such as orbital drift, calibration loss and
186 volcanic eruptions (Beck et al., 2011; Pinzon and Tucker, 2014). For the current study, the latest version of
187 GIMMS NDVI (3g.v1) was used, which covers the time period from 1981 to 2015 at biweekly temporal
188 resolution and 8-km spatial resolution (Pinzon and Tucker, 2014).

189 2.3 Methods

190 2.3.1 SPEI calculation

191 The SPEI proposed by Vicente-Serrano et al. (2010) has been used for a wide variety of agricultural,
192 ecological and hydro-meteorological applications (e.g., Jiang et al., 2019; Naumann et al., 2018; Schwalm et
193 al., 2017). It accounts for the impacts of evaporation demand on droughts and inherits the simplicity and
194 multi-temporal characteristics of SPI. The procedure for SPEI calculation includes the estimation of a
195 climatic water balance (namely the difference between precipitation and potential evaporation), the
196 aggregation of the climatic water balance over various time-scales (e.g., 1, 3, 6, 12, 24, or more months), and
197 a fitting to a certain parameter distribution. As suggested by Beguería et al. (2014) and Vicente-Serrano and
198 Beguería (2016), the log-logistic probability distribution is best for SPEI calculation, from which the
199 probability distribution of the difference between precipitation and potential evaporation can be calculated as
200 suggested by Vicente-Serrano et al. (2010) and Beguería et al. (2014). The negative and positive SPEI values
201 respectively indicate dry and wet conditions. In this study, the CHIRPS and GLEAM datasets were used for
202 SPEI calculation at high spatial resolution (5-km). For comparison, the SPEI at 50-km was also calculated
203 based on CRU TS datasets for the same 1981–2016 period. It should be noted that the SPEI over sparsely
204 vegetated and barren areas were masked out based on Moderate Resolution Imaging Spectroradiometer
205 (MODIS) land cover product (MCD12Q1) (Friedl et al., 2010), because SPEI is not reliable over these areas
206 (Beguería et al., 2010; Beguería et al., 2014; Zhao et al., 2017).

207 2.3.2 Evaluation criteria



208 The SPEIbase dataset (Beguería et al., 2010) was calculated with CRU TS dataset, which has been evaluated
209 and applied by many studies (e.g., Chen et al., 2013; Greenwood et al., 2017; Isbell et al., 2015; Sun et al.,
210 2016a; Um et al., 2017; Vicente-Serrano et al., 2013) The newly-generated SPEI at high spatial resolution
211 based on CHIRPS and GLEAM (SPEI-HR) is compared temporally and spatially with the SPEI calculated
212 from CRU TS datasets. In addition, the NDVI can also serve as an indicator for drought and vegetation
213 health, and to assess the performance of drought indices (Aadhar and Mishra, 2017; Vicente-Serrano et al.,
214 2013). Furthermore, root zone soil moisture is an ideal hydrological variable for agricultural (soil moisture)
215 drought monitoring. The recently-released root zone soil moisture (RSM) from GLEAM v3 provides a great
216 opportunity to evaluate whether soil moisture drought is well represented by SPEI. To facilitate direct
217 comparison between SPEI and NDVI as well as RSM, both NDVI and RSM are standardized by subtracting
218 their corresponding (1981–2016) mean and expressed the resulting anomalies as numbers of standard
219 deviations. This standardization has been applied by many studies to evaluate drought indices (Anderson et
220 al., 2011; Mu et al., 2013; Zhao et al., 2017). The correlation between SPEI and the standardized NDVI and
221 RSM is quantified using Pearson’s correlation coefficient (R). In addition, the high resolution SPEI from
222 GLEAM and CHIRPS is also resampled to the same grid size of SPEI from CRU TS in order to quantify
223 their correlation and disentangle whether the added value of the former arises from its increased accuracy or
224 higher resolution. In the following part, the high (5-km) resolution SPEI is referred to SPEI-HR, while the
225 coarse 50-km resolution SPEI is referred to SPEI-CRU.

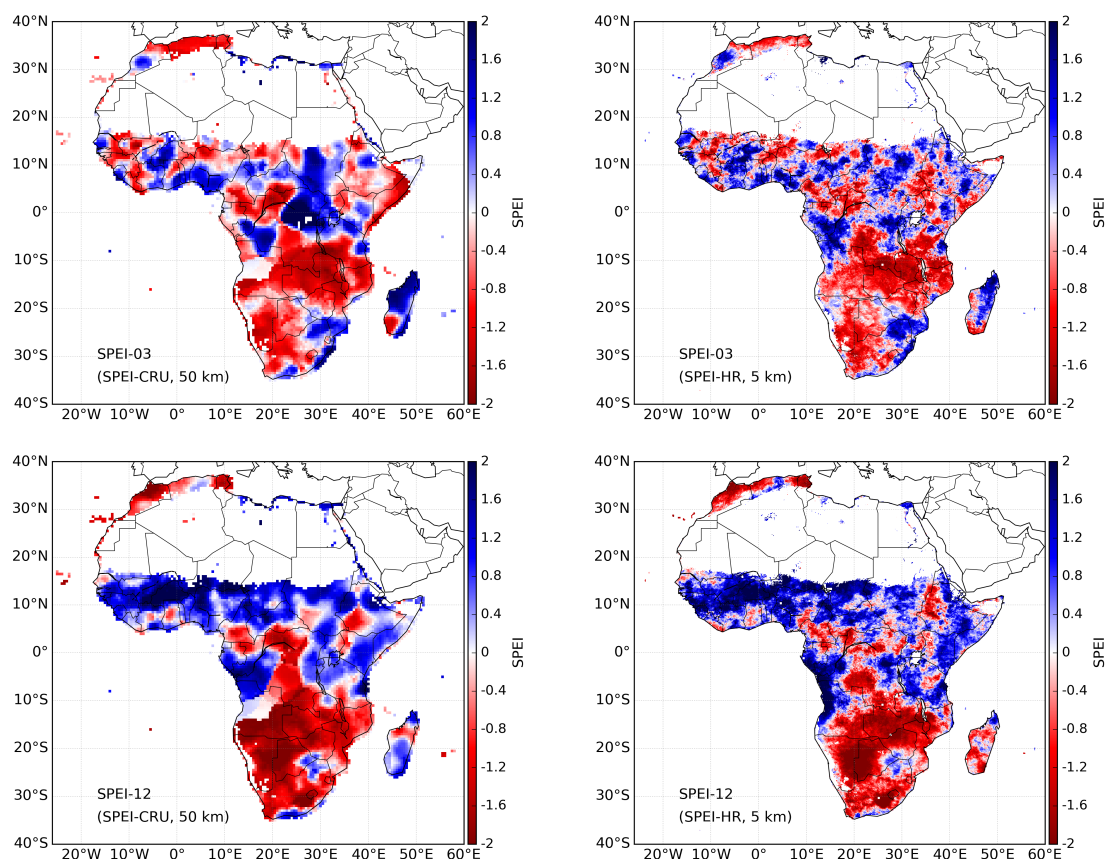
226 **3 Results and discussion**

227 **3.1 Inter-comparison between high- and coarse-resolution SPEI**

228 Figure 1 shows the spatial distribution of SPEI-HR and SPEI-CRU at different resolutions for an example
229 month (June 1995). Figure 1a,b show the 3-month SPEI and 12-month SPEI, respectively. It can be seen that
230 the high resolution and coarse resolution SPEI display quite similar dry and wet patterns over the whole of
231 Africa for both temporal scales. However, as expected, the SPEI-HR shows much more spatial detail that
232 reflects mesoscale geographic and climatic features, which highlights the advantages of this new dataset. The



233 differences in patterns between 3-month and 12-month SPEI indicate the different water deficits caused by
234 different aggregation time scales, which can further separate agricultural, hydrological, environmental, and
235 other droughts. For example, in June 1995 southern Africa showed persistent dry conditions over a
236 prolonged period, while western Africa only showed a short-term drought.



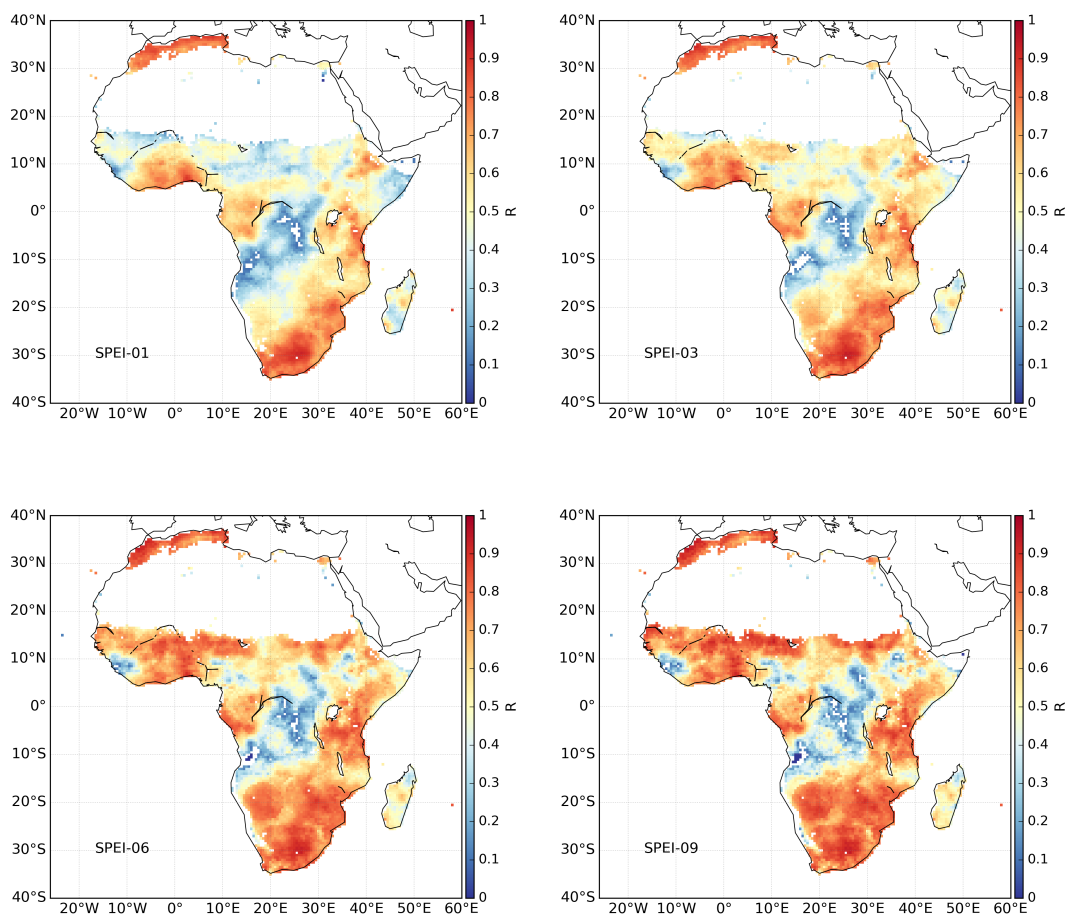
237
238
239
240
241

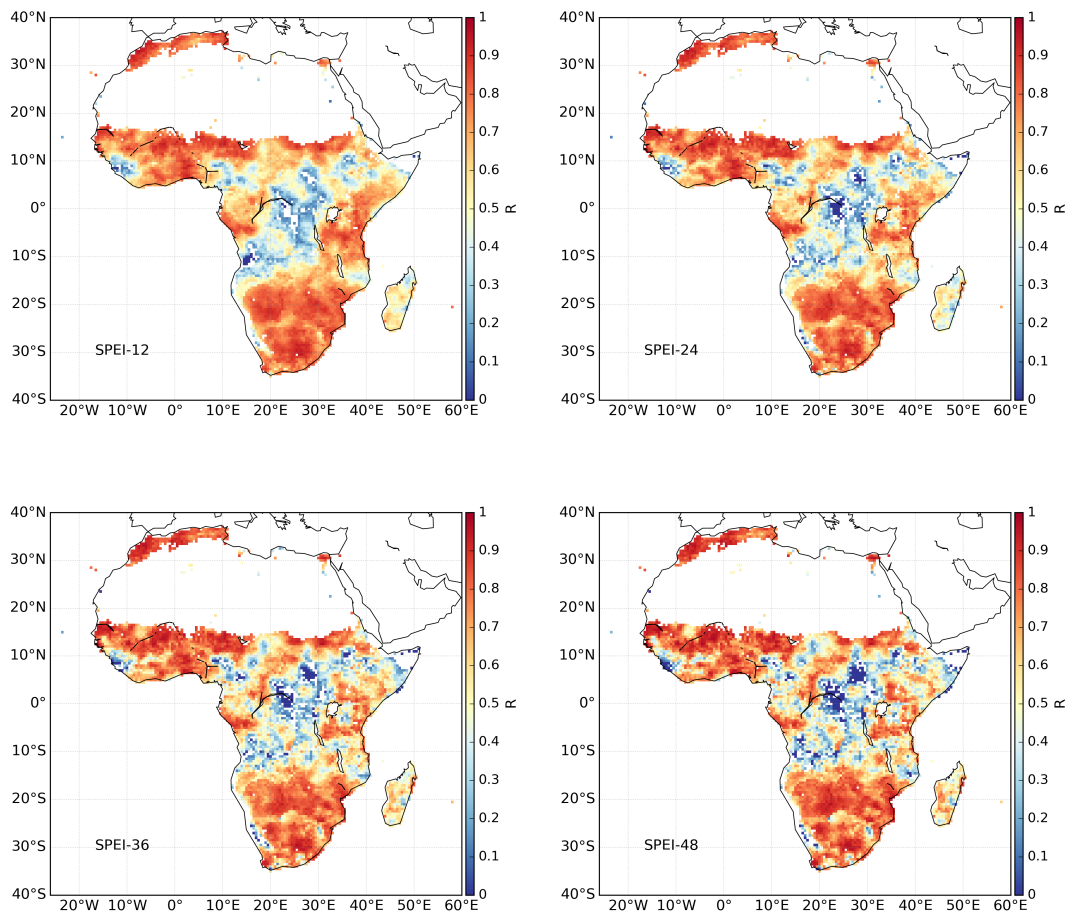
Figure 1: Spatial patterns of 3-month and 12-month SPEI at high spatial resolution (5 km) and coarse spatial resolution (50 km) in June, 1995. The high spatial resolution SPEI (SPEI-HR) is based on CHIRPS precipitation and GLEAM potential evaporation, while the coarse spatial resolution SPEI (SPEI-CRU) is calculated from CRU TS datasets.

242 In order to quantify how different is SPEI-HR from SPEI-CRU, the correlation between them is calculated
243 for each grid cell over the whole study period. Figure 2 shows the correlations for time-scales 1, 3, 6, 9, 12,
244 24, 36, and 48 months. In general, the SPEI-HR and SPEI-CRU agree well in terms of temporal variability
245 with high positive correlations over most of Africa for every time scale. However, relatively low correlations
246 appear in central Africa, and they become lower as the SPEI time-scale increases. This region has very few



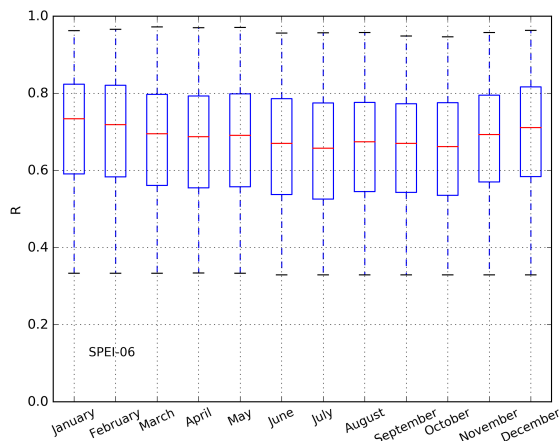
247 station observations. It should be noted that the correlations shown here are statistically significant with p
248 value less than 0.05. In addition, the average correlation between 6-month SPEI-CRU and SPEI-HR for
249 each month of the year is summarized in Figure 3 using box plot. In general, positive correlations, with a
250 median larger than 0.6 ($p < 0.05$), are found for every month. There are no substantial differences in
251 correlations between different months. Figure A1 in Appendix shows additional box plots for SPEI at other
252 time scales.





253
254
255

Figure 2: Correlation ($p < 0.05$) between SPEI-HR and SPEI-CRU, with the number indicating different months.



256
257
258
259

Figure 3: Box plot of the correlation ($p < 0.05$) between SPEI-HR and SPEI-CRU for each month of the entire record. The results here are based on 6-month SPEI and the red line in each box represents the median.

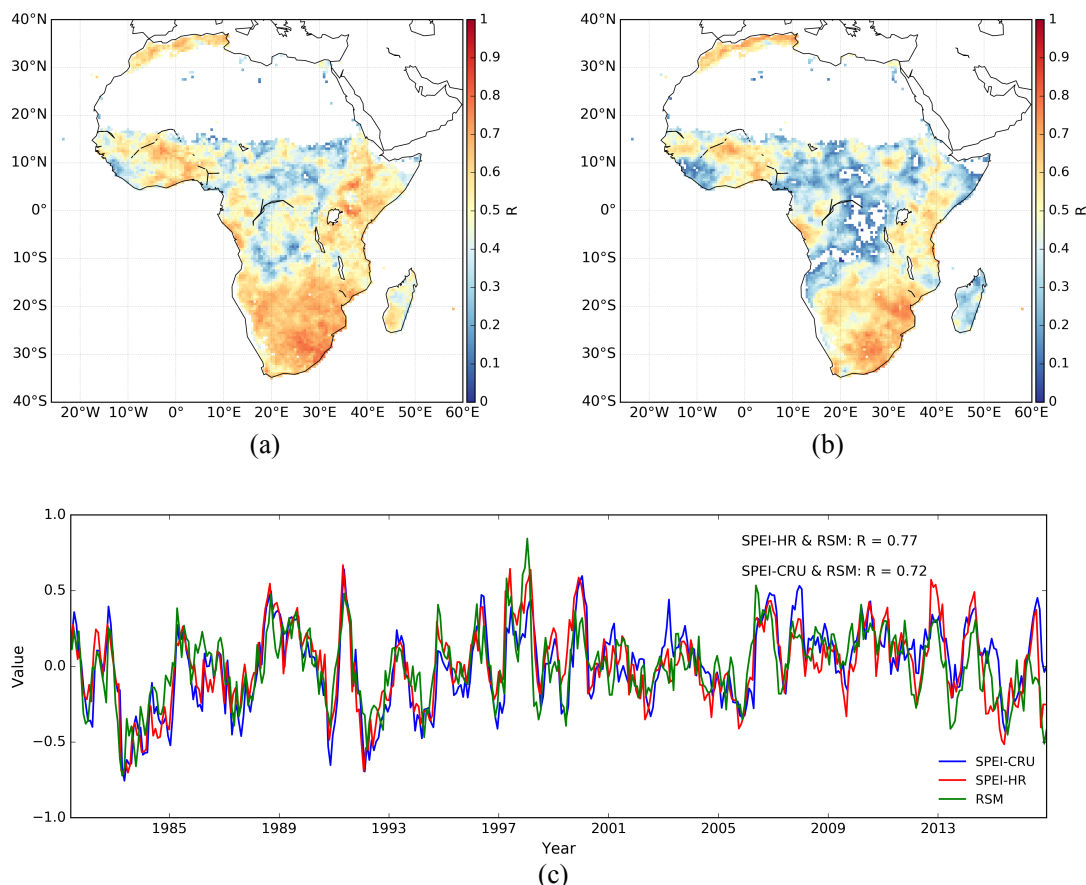


260

261 3.2 Comparison against root zone soil moisture and NDVI

262 To gain more insights into their significance and applicability, the SPEI datasets are compared with NDVI
263 and RSM. Figure 4 shows the results of the spatial and temporal comparison between 6-month SPEI and
264 RSM as indicated by Törnros and Menzel (2014). Figure 4a,b display the correlation ($p < 0.05$) of SPEI-HR
265 and SPEI-CRU against RSM during the whole time period respectively. In general, both SPEI-HR and SPEI-
266 CRU show strong correlations with RSM over the whole African continent. Compared to SPEI-CRU, the
267 SPEI-HR shows higher correlations, particularly over central Africa. Since Section 3.1 shows that relatively
268 large discrepancy between SPEI-CRU and SPEI-HR exists over central Africa, the results presented here
269 suggest a potentially better performance of SPEI-HR compared with SPEI-CRU in this region.

270 The time series of SPEI and RSM, averaged over the entire study area, are shown in Figure 4c, together with
271 the corresponding correlations. It can be seen that both SPEI-HR and SPEI-CRU agree well with each other
272 and with the RSM dynamics. Consistent with the results from the spatial correlation analysis, the SPEI-HR
273 and SPEI-CRU show similar results when compared with RSM ($R = 0.77$ for SPEI-HR, $R = 0.72$ for SPEI-
274 CRU). Furthermore, the scatterplots between 6-month SPEI and RSM for the entire data record are shown in
275 Appendix Figure A2, where positive and significant correlations with RSM are found for both SPEI-HR ($R =$
276 0.51) and SPEI-CRU ($R = 0.42$). To explore the correlation between RSM and different time scales of SPEI,
277 Table 1 summarizes the correlation value calculated in the same way as Figure 4c. It can be seen that the
278 highest correlations against RSM are found at 3- and 6-month time scales. It should be noted that satellite
279 data-driven estimates of root zone soil moisture is more suitable for evaluating SPEI compared to satellite-
280 based top-layer soil moisture or reanalysis soil moisture data (Mo et al., 2011; Xu et al., 2018).



281 Figure 4: Spatial maps of correlation between SPEI and root zone soil moisture (RSM) for 6-month SPEI: (a) SPEI-HR and (b)
 282 SPEI-CRU. The time series of Africa area-mean RSM and SPEI are shown in (c), where R refers to the correlation coefficient.
 283 The correlations shown here are all significant at the 95% confidence level.
 284
 285

286 Table 1: The correlation ($p < 0.05$) between area-mean RSM and SPEI at different time scales.
 287

	SPEI-01	SPEI-03	SPEI-06	SPEI-09	SPEI-12	SPEI-24	SPEI-36	SPEI-48
R (SPEI-CRU)	0.52	0.74	0.72	0.64	0.56	0.41	0.26	0.16
R (SPEI-HR)	0.49	0.76	0.77	0.69	0.62	0.44	0.29	0.18

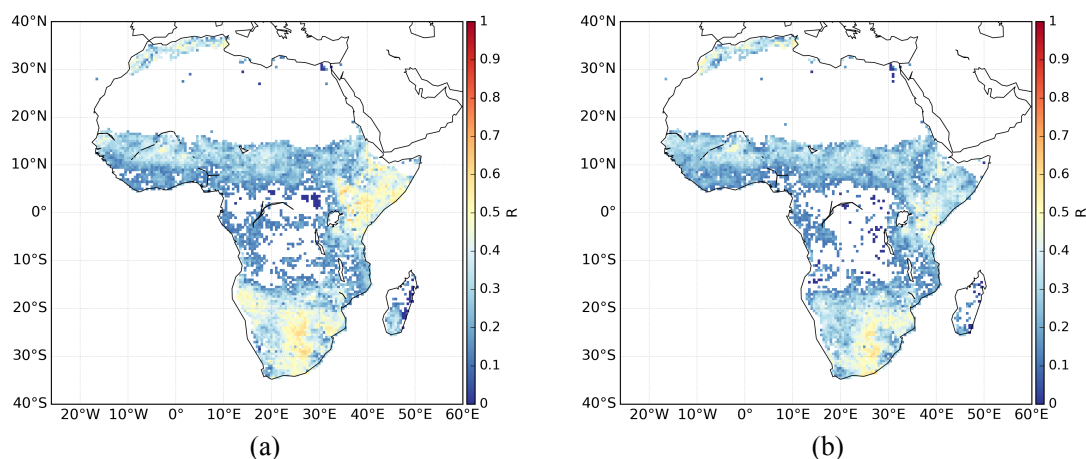
288

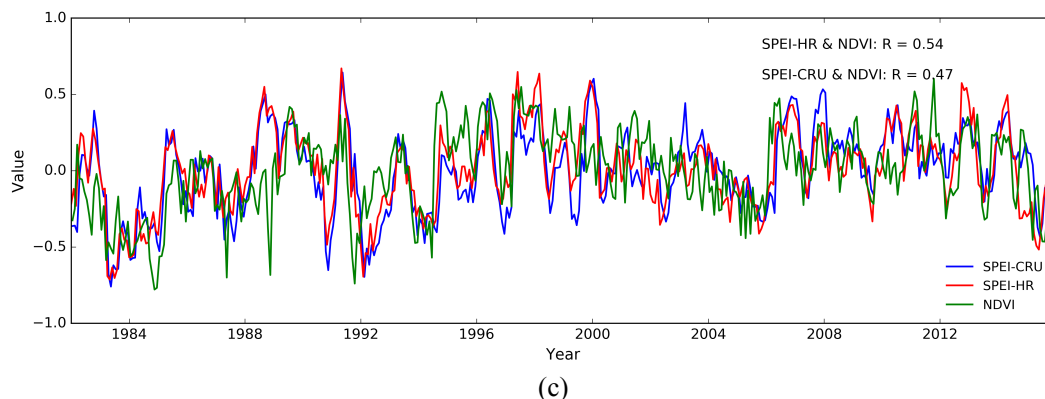
289 Similar to the above analysis between SPEI and RSM, the comparison of results between SPEI and NDVI
 290 are shown in Figure 5. First, Figures 5a,b present the spatial distribution of the correlations ($p < 0.05$) between
 291 SPEI-HR and NDVI and between SPEI-CRU and NDVI, respectively. While correlations are overall lower
 292 than for RSM, it can be seen that both SPEI datasets are positively correlated with NDVI over most of the
 293 continent. It is also clear that SPEI-HR shows higher correlations. The time series comparison between the



294 area-mean SPEI and NDVI is shown in Figure 5c. Both SPEI-HR and SPEI-CRU show agreement with
295 NDVI, with $R=0.54$ and $R=0.47$, respectively. In addition, the comparison between 6-month SPEI and
296 NDVI for the entire data record was also calculated, with $R=0.24$ for SPEI-HR and $R=0.21$ for SPEI-CRU
297 significant at 95% confidence level (Figure A3). While these correlations are admittedly low, overall results
298 suggest that the SPEI has a positive relation with NDVI, which is also reported by previous studies (e.g.,
299 Törnros and Menzel, 2014; Vicente-Serrano et al., 2018). The lower correlations against NDVI than against
300 RSM are likely due to complex physiological processes associated to vegetation, and the fact that ecosystem
301 state is driven by multiple variables other than water availability (Nemani et al., 2003). Furthermore, there
302 are also clearly documented lags between precipitation and NDVI, with NDVI time series typically peaking
303 one or even two months after the period of maximum rainfall (Funk and Brown, 2006). Finally, Table 2
304 summarizes the correlation between SPEI and NDVI at different time scales. Compared with the results
305 presented in Table 1 for RSM, the correlation with NDVI shown in Table 2 is also generally lower, and the
306 highest correlations appear between 9- and 24-month SPEI ($R>0.5$).

307
308
309
310





311
 312
 313
 314
 315
 316
 317
 318
 319

Figure 5: Spatial maps of the correlation between SPEI and NDVI for 6-month SPEI: (a) SPEI-HR and (b) SPEI-CRU. The time series of area-mean NDVI and SPEI are shown in (c), where R refers to the correlation coefficient. The correlations shown here are all significant at the 95% confidence level.

Table 2: The correlation ($p < 0.05$) between area-mean NDVI and SPEI at different time scales.

	SPEI-01	SPEI-03	SPEI-06	SPEI-09	SPEI-12	SPEI-24	SPEI-36	SPEI-48
R (SPEI-CRU)	0.23	0.42	0.47	0.48	0.47	0.50	0.34	0.20
R (SPEI-HR)	0.31	0.51	0.54	0.56	0.57	0.57	0.44	0.29

320

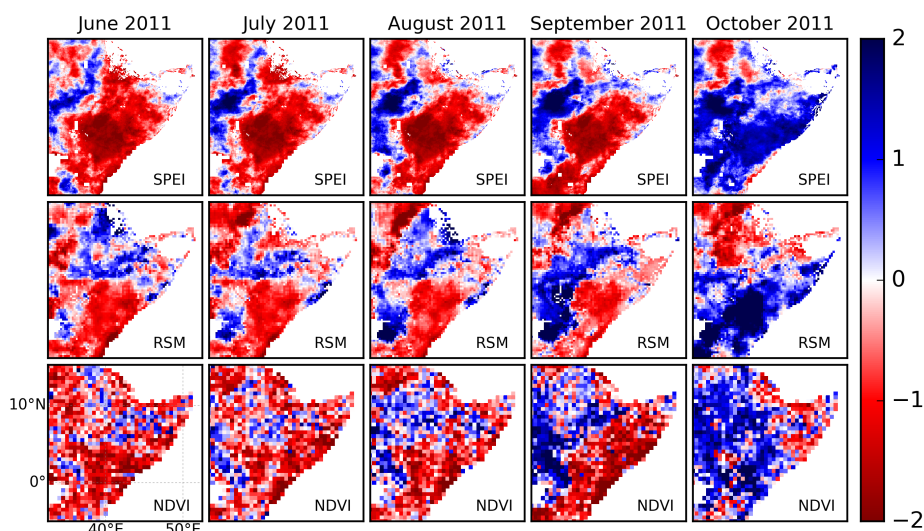
321 Altogether, the comparisons between SPEI and RSM and between SPEI and NDVI indirectly indicate the
 322 validity of the generated SPEI datasets. Therefore, the generated high-resolution SPEI-HR from satellite
 323 products has potential to improve upon the state of the art in drought assessment over Africa.

324 3.3 Patterns of SPEI, RSM and NDVI during specific drought events

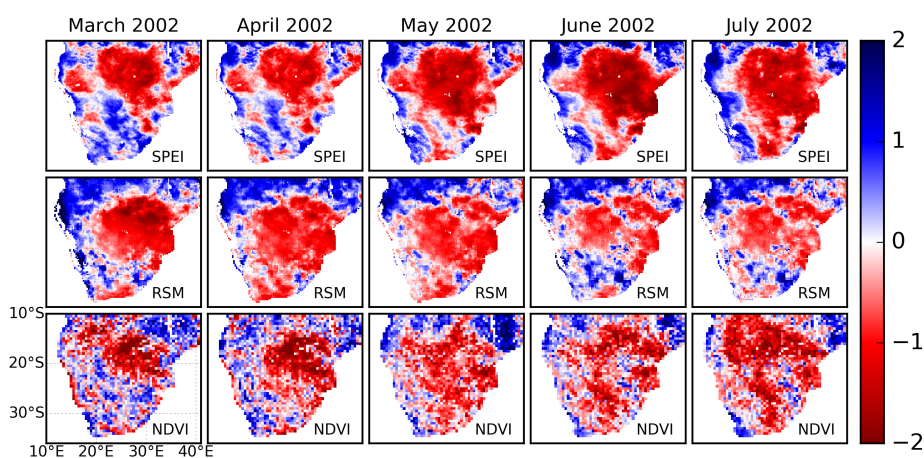
325 Most of Africa has suffered severe droughts in past decades (Blamey et al., 2018; Naumann et al., 2014).
 326 Among them, the 2011 East Africa drought (AghaKouchak, 2015; Anderson et al., 2012) and 2002 southern
 327 Africa drought (Masih et al., 2014) were extremely severe and had devastating effects on the natural and
 328 socioeconomic environment. Taking these two events as case studies, the spatial patterns of the newly-
 329 developed high-resolution 6-month SPEI-HR are analyzed, together with the variability in NDVI and RSM.
 330 Figure 6a,b show the evolution of 6-month SPEI, NDVI and RSM during the 2011 East Africa and the 2002
 331 southern Africa drought, respectively. The 6-month periods end in the named month, with the 6-month June
 332 2011 SPEI values based on data for January to June. In general, these three variables reflect the progressive



333 dry-out during the events. For example, strong, severe drought is revealed by the SPEI with values less than
334 -1.5, coinciding with a decline in NDVI and RSM, from June to September 2011 over East Africa; the
335 drought was offset in October. Similarly, dry and wet conditions variations during the 2002 southern Africa
336 drought were also captured by the three variables. Despite differences over space and time, results here
337 demonstrate that the generated SPEI-HR captures the main drought conditions that are reflected by negative
338 anomalies in NDVI and RSM, and can thus be used to study local drought related processes and societal
339 impacts in Africa.



(a)



(b)



341 Figure 6: Evolution of the spatial patterns of 6-month SPEI-HR, NDVI and root zone soil moisture (RSM) during the 2011 East
342 Africa drought (a) and 2002 southern Africa drought (b), respectively.

343
344

345 **4. Data availability**

346 The high resolution SPEI dataset is publically available from the Centre for Environmental Data Analysis
347 (CEDA) with link: <http://dx.doi.org/10.5285/bbdfd09a04304158b366777eba0d2aeb> (Peng et al., 2019a). It
348 covers the whole Africa at monthly temporal resolution and 5 km spatial resolution from 1981 to 2016, and
349 is provided with Geographic Lat/Lon projection and NetCDF format.

350

351 **5. Conclusion**

352 The study presents a newly-generated high-resolution SPEI dataset (SPEI-HR) over Africa. The dataset is
353 produced from satellite-based CHIRPS precipitation and GLEAM potential evaporation, and covers the
354 entire African continent over the time period from 1981 to 2016 with spatial resolution of 5-km. The
355 accumulated SPEI ranging from 1 to 48 months is provided to facilitate applications from meteorological to
356 hydrological droughts. The SPEI-HR was compared with widely used coarse-resolution SPEI data (SPEI-
357 CRU) and GIMMS NDVI as well as GLEAM root zone soil moisture to investigate its capability for drought
358 detection. In general, the SPEI-HR has good correlation with SPEI-CRU temporally and spatially. They both
359 agree well with NDVI and root zone soil moisture, although SPEI-HR displays higher correlations overall.
360 These results indicate the validity and advantage of the newly developed high resolution SPEI-HR dataset,
361 and its unprecedentedly high spatial resolution offers important advantages for drought monitoring and
362 assessment at district and river basin level in Africa.

363

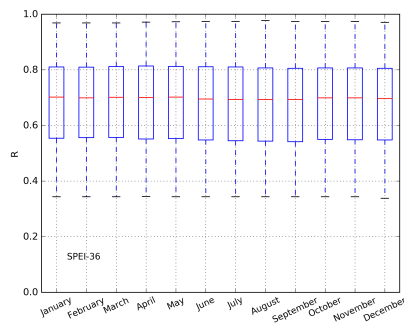
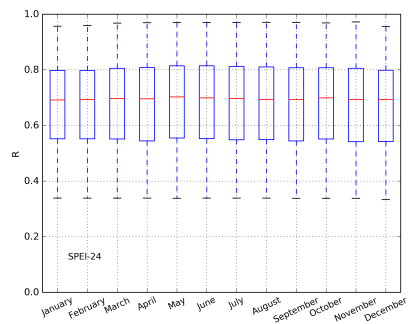
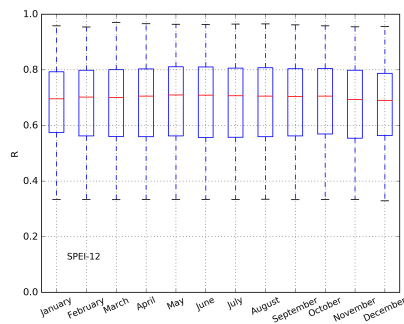
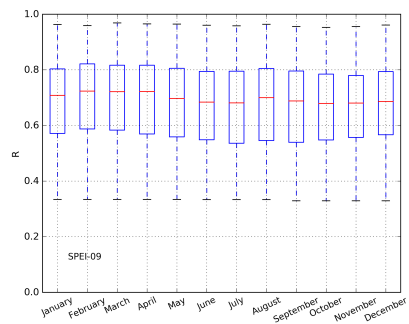
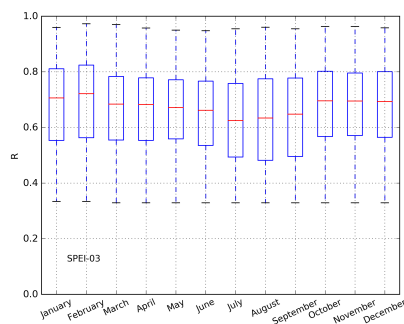
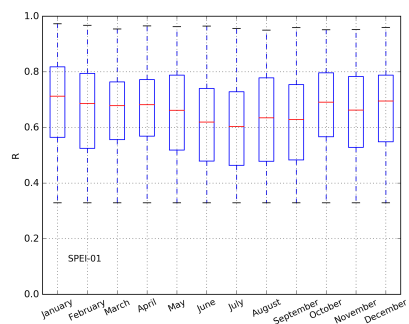
364

365



366

367 Appendix





368

369

370

371

372

373

374

375

376

377

378

379

380

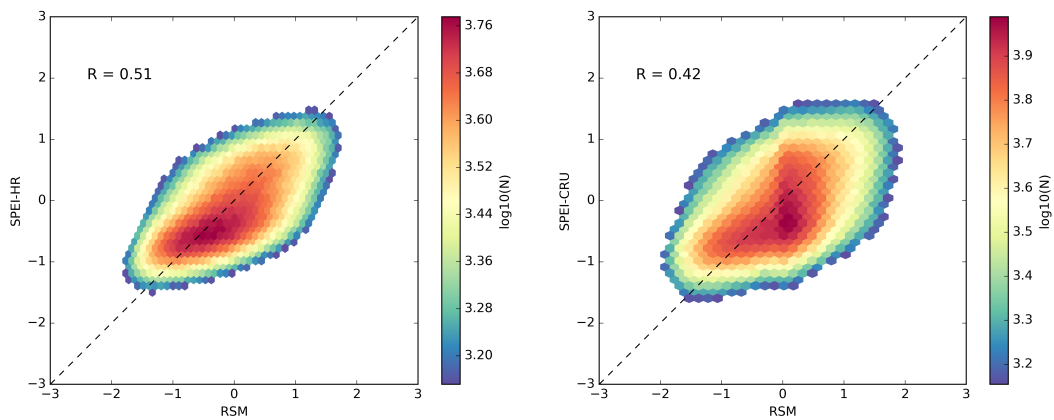
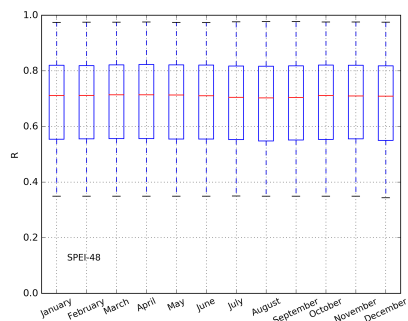
381

Figure A1: Box plots of the correlation ($p < 0.05$) between SPEI-HR and SPEI-CRU for each month and entire monthly record.

382

383

384



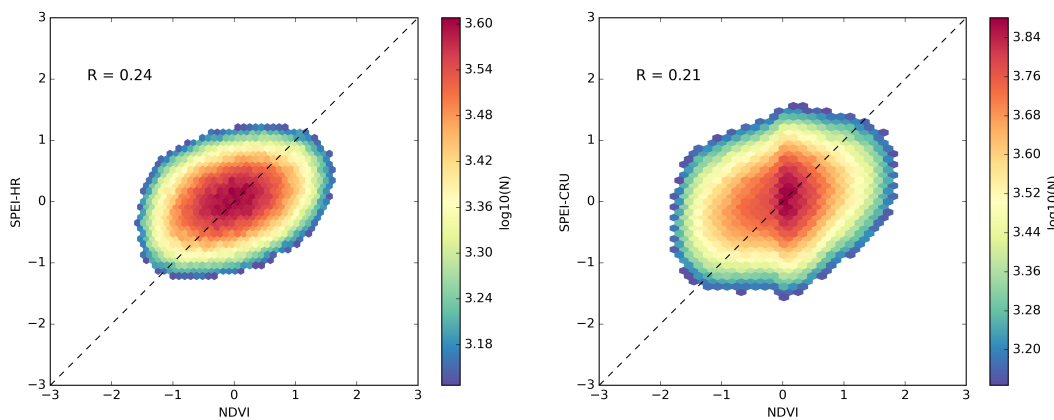
385

Figure A2: Scatterplots between 6-month SPEI and RSM for the entire data record. R is correlation coefficient with $p < 0.05$, and the colors denote the occurrence frequency of values.

386

387

388





389 Figure A3: Scatterplots between 6-month SPEI and NDVI for the entire data record. R is correlation coefficient with $p < 0.05$, and
390 the colors denote the occurrence frequency of values.
391

392 **Acknowledgments**

393 This work is supported by the UK Space Agency's International Partnership Programme (417000001429).
394 D.G.M. acknowledges funding from the European Research Council (ERC) under grant agreement 715254
395 (DRY-2-DRY). SD is also funded by the Natural Environment Research Council (NE/M020339/1). CF is
396 supported by the U.S. Geological Survey's Drivers of Drought program and NASA Harvest Program grant
397 Z60592017.

398



399

400

401 References

- 402 Aadhar, S. and Mishra, V.: High-resolution near real-time drought monitoring in South Asia, *Scientific data*, 4, 170145, 2017.
- 403 Adler, R. F., Huffman, G. J., Chang, A., Ferraro, R., Xie, P.-P., Janowiak, J., Rudolf, B., Schneider, U., Curtis, S., Bolvin, D.,
404 Gruber, A., Susskind, J., Arkin, P., and Nelkin, E.: The Version-2 Global Precipitation Climatology Project (GPCP) Monthly
405 Precipitation Analysis (1979–Present), *Journal of Hydrometeorology*, 4, 1147-1167, 2003.
- 406 AghaKouchak, A.: A multivariate approach for persistence-based drought prediction: Application to the 2010–2011 East Africa
407 drought, *Journal of Hydrology*, 526, 127-135, 2015.
- 408 AghaKouchak, A., Farahmand, A., Melton, F. S., Teixeira, J., Anderson, M. C., Wardlow, B. D., and Hain, C. R.: Remote sensing
409 of drought: Progress, challenges and opportunities, *Reviews of Geophysics*, 53, 452-480, 2015.
- 410 Anderson, M. C., Hain, C., Wardlow, B., Pimstein, A., Mecikalski, J. R., and Kustas, W. P.: Evaluation of drought indices based
411 on thermal remote sensing of evapotranspiration over the continental United States, *Journal of Climate*, 24, 2025-2044, 2011.
- 412 Anderson, W. B., Zaitchik, B. F., Hain, C. R., Anderson, M. C., Yilmaz, M. T., Mecikalski, J., and Schultz, L.: Towards an
413 integrated soil moisture drought monitor for East Africa, *Hydrol. Earth Syst. Sci.*, 16, 2893-2913, 2012.
- 414 Anghileri, D., Li, C., Agaba, G., Kandel, M., Dash, J., Reeves, J., Lewis, L., Hill, C., and Sheffield, J.: Co-production and
415 interdisciplinary research in the BRECCIA project: bringing together different expertise and actors for addressing water and
416 food security challenges in sub-Saharan Africa, *Geophysical Research Abstracts*, EGU2019-14992.
- 417 Arpe, K., Leroy, S., Lahijani, H., and Khan, V.: Impact of the European Russia drought in 2010 on the Caspian Sea level,
418 *Hydrology and earth system science*, 16, 19-27, 2012.
- 419 Awange, J. L., Khandu, Schumacher, M., Forootan, E., and Heck, B.: Exploring hydro-meteorological drought patterns over the
420 Greater Horn of Africa (1979–2014) using remote sensing and reanalysis products, *Advances in Water Resources*, 94, 45-59,
421 2016.
- 422 Bachmair, S., Stahl, K., Collins, K., Hannaford, J., Acreman, M., Svoboda, M., Knutson, C., Smith, K. H., Wall, N., and Fuchs,
423 B.: Drought indicators revisited: the need for a wider consideration of environment and society, *Wiley Interdisciplinary
424 Reviews: Water*, 3, 516-536, 2016.
- 425 Bachmair, S., Tanguy, M., Hannaford, J., and Stahl, K.: How well do meteorological indicators represent agricultural and forest
426 drought across Europe?, *Environmental Research Letters*, 13, 034042, 2018.
- 427 Baudoin, M.-A., Vogel, C., Nortje, K., and Naik, M.: Living with drought in South Africa: lessons learnt from the recent El Niño
428 drought period, *International Journal of Disaster Risk Reduction*, 23, 128-137, 2017.
- 429 Beck, H. E., McVicar, T. R., van Dijk, A. I., Schellekens, J., de Jeu, R. A., and Bruijnzeel, L. A.: Global evaluation of four
430 AVHRR–NDVI data sets: Intercomparison and assessment against Landsat imagery, *Remote Sensing of Environment*, 115,
431 2547-2563, 2011.
- 432 Beck, H. E., Van Dijk, A. I., Levizzani, V., Schellekens, J., Gonzalez Miralles, D., Martens, B., and De Roo, A.: MSWEP: 3-
433 hourly 0.25 global gridded precipitation (1979-2015) by merging gauge, satellite, and reanalysis data, *Hydrology and Earth
434 System Sciences*, 21, 589-615, 2017.
- 435 Becker, A., Finger, P., Meyer-Christoffer, A., Rudolf, B., Schamm, K., Schneider, U., and Ziese, M.: A description of the global
436 land-surface precipitation data products of the Global Precipitation Climatology Centre with sample applications including
437 centennial (trend) analysis from 1901–present, *Earth System Science Data*, 5, 71-99, 2013.
- 438 Beguería, S., Vicente-Serrano, S. M., and Angulo-Martínez, M.: A multiscalar global drought dataset: the SPEIbase: a new
439 gridded product for the analysis of drought variability and impacts, *Bulletin of the American Meteorological Society*, 91, 1351-
440 1356, 2010.
- 441 Beguería, S., Vicente-Serrano, S. M., Reig, F., and Latorre, B.: Standardized precipitation evapotranspiration index (SPEI)
442 revisited: parameter fitting, evapotranspiration models, tools, datasets and drought monitoring, *International Journal of
443 Climatology*, 34, 3001-3023, 2014.
- 444 Blamey, R. C., Kolusu, S. R., Mahlalela, P., Todd, M. C., and Reason, C. J. C.: The role of regional circulation features in
445 regulating El Niño climate impacts over southern Africa: A comparison of the 2015/2016 drought with previous events,
446 *International Journal of Climatology*, 0, 2018.
- 447 Chadwick, R., Good, P., Martin, G., and Rowell, D. P.: Large rainfall changes consistently projected over substantial areas of
448 tropical land, *Nature Climate Change*, 6, 177, 2015.
- 449 Chen, T., Werf, G. R., Jeu, R. A. M., Wang, G., and Dolman, A. J.: A global analysis of the impact of drought on net primary
450 productivity, *Hydrol. Earth Syst. Sci.*, 17, 3885-3894, 2013.
- 451 Crausbay, S. D., Ramirez, A. R., Carter, S. L., Cross, M. S., Hall, K. R., Bathke, D. J., Betancourt, J. L., Colt, S., Cravens, A. E.,
452 and Dalton, M. S.: Defining ecological drought for the twenty-first century, *Bulletin of the American Meteorological Society*,
453 98, 2543-2550, 2017.



- 454 Delworth, T. L., Zeng, F., Rosati, A., Vecchi, G. A., and Wittenberg, A. T.: A Link between the Hiatus in Global Warming and
455 North American Drought, *Journal of Climate*, 28, 3834-3845, 2015.
- 456 Deo, R. C., Byun, H.-R., Adamowski, J. F., and Begum, K.: Application of effective drought index for quantification of
457 meteorological drought events: a case study in Australia, *Theoretical and Applied Climatology*, 128, 359-379, 2017.
- 458 Ding, Y., Hayes, M. J., and Widhalm, M.: Measuring economic impacts of drought: a review and discussion, *Disaster Prevention
459 and Management: An International Journal*, 20, 434-446, 2011.
- 460 Dinku, T., Funk, C., Peterson, P., Maidment, R., Tadesse, T., Gadain, H., and Ceccato, P.: Validation of the CHIRPS satellite
461 rainfall estimates over eastern Africa, *Quarterly Journal of the Royal Meteorological Society*, 0, 2018.
- 462 Duan, Z., Liu, J., Tuo, Y., Chiogna, G., and Disse, M.: Evaluation of eight high spatial resolution gridded precipitation products in
463 Adige Basin (Italy) at multiple temporal and spatial scales, *Science of The Total Environment*, 573, 1536-1553, 2016.
- 464 Fan, Y. and Van den Dool, H.: A global monthly land surface air temperature analysis for 1948–present, *Journal of Geophysical
465 Research: Atmospheres*, 113, 2008.
- 466 Fisher, J. B., Melton, F., Middleton, E., Hain, C., Anderson, M., Allen, R., McCabe, M. F., Hook, S., Baldocchi, D., and
467 Townsend, P. A.: The future of evapotranspiration: Global requirements for ecosystem functioning, carbon and climate
468 feedbacks, agricultural management, and water resources, *Water Resources Research*, 53, 2618-2626, 2017.
- 469 Forzieri, G., Alkama, R., Miralles, D. G., and Cescatti, A.: Satellites reveal contrasting responses of regional climate to the
470 widespread greening of Earth, *Science*, 356, 1180-1184, 2017.
- 471 Friedl, M. A., Sulla-Menashe, D., Tan, B., Schneider, A., Ramankutty, N., Sibley, A., and Huang, X.: MODIS Collection 5 global
472 land cover: Algorithm refinements and characterization of new datasets, *Remote sensing of Environment*, 114, 168-182, 2010.
- 473 Funk, C., Harrison, L., Shukla, S., Pomposi, C., Galu, G., Korecha, D., Husak, G., Magadzire, T., Davenport, F., and Hillbruner,
474 C.: Examining the role of unusually warm Indo-Pacific sea-surface temperatures in recent African droughts, *Quarterly Journal
475 of the Royal Meteorological Society*, 144, 360-383, 2018.
- 476 Funk, C., Peterson, P., Landsfeld, M., Pedreros, D., Verdin, J., Shukla, S., Husak, G., Rowland, J., Harrison, L., Hoell, A., and
477 Michaelsen, J.: The climate hazards infrared precipitation with stations—a new environmental record for monitoring extremes,
478 *Scientific Data*, 2, 150066, 2015a.
- 479 Funk, C., Verdin, A., Michaelsen, J., Peterson, P., Pedreros, D., and Husak, G.: A global satellite-assisted precipitation
480 climatology, *Earth Syst. Sci. Data*, 7, 275-287, 2015e.
- 481 Funk, C. C. and Brown, M. E.: Intra-seasonal NDVI change projections in semi-arid Africa, *Remote Sensing of Environment*, 101,
482 249-256, 2006.
- 483 Funk, C. C., Peterson, P. J., Landsfeld, M. F., Pedreros, D. H., Verdin, J. P., Rowland, J. D., Romero, B. E., Husak, G. J.,
484 Michaelsen, J. C., and Verdin, A. P.: A quasi-global precipitation time series for drought monitoring, *US Geological Survey
485 Data Series*, 832, 2014.
- 486 García-Herrera, R., Díaz, J., Trigo, R. M., Luterbacher, J., and Fischer, E. M.: A review of the European summer heat wave of
487 2003, *Critical Reviews in Environmental Science and Technology*, 40, 267-306, 2010.
- 488 Greenwood, S., Ruiz-Benito, P., Martínez-Vilalta, J., Lloret, F., Kitzberger, T., Allen, C. D., Fensham, R., Laughlin, D. C., Kattge,
489 J., and Bönisch, G.: Tree mortality across biomes is promoted by drought intensity, lower wood density and higher specific
490 leaf area, *Ecology Letters*, 20, 539-553, 2017.
- 491 Greve, P., Orlowsky, B., Mueller, B., Sheffield, J., Reichstein, M., and Seneviratne, S. I.: Global assessment of trends in wetting
492 and drying over land, *Nature geoscience*, 7, 716, 2014.
- 493 Griffin, D. and Anchukaitis, K. J.: How unusual is the 2012–2014 California drought?, *Geophysical Research Letters*, 41, 9017-
494 9023, 2014.
- 495 Harris, I., Jones, P. D., Osborn, T. J., and Lister, D. H.: Updated high-resolution grids of monthly climatic observations – the CRU
496 TS3.10 Dataset, *International Journal of Climatology*, 34, 623-642, 2014.
- 497 Heim Jr, R. R.: A review of twentieth-century drought indices used in the United States, *Bulletin of the American Meteorological
498 Society*, 83, 1149-1165, 2002.
- 499 Isbell, F., Craven, D., Connolly, J., Loreau, M., Schmid, B., Beierkuhnlein, C., Bezemer, T. M., Bonin, C., Bruelheide, H., de
500 Luca, E., Ebeling, A., Griffin, J. N., Guo, Q., Hautier, Y., Hector, A., Jentsch, A., Kreyling, J., Lanta, V., Manning, P., Meyer,
501 S. T., Mori, A. S., Naeem, S., Niklaus, P. A., Polley, H. W., Reich, P. B., Roscher, C., Seabloom, E. W., Smith, M. D., Thakur,
502 M. P., Tilman, D., Tracy, B. F., van der Putten, W. H., van Ruijven, J., Weigelt, A., Weisser, W. W., Wilsey, B., and
503 Eisenhauer, N.: Biodiversity increases the resistance of ecosystem productivity to climate extremes, *Nature*, 526, 574, 2015.
- 504 Jägermeyr, J., Gerten, D., Schaphoff, S., Heinke, J., Lucht, W., and Rockström, J.: Integrated crop water management might
505 sustainably halve the global food gap, *Environmental Research Letters*, 11, 025002, 2016.
- 506 Jiang, P., Liu, H., Piao, S., Ciais, P., Wu, X., Yin, Y., and Wang, H.: Enhanced growth after extreme wetness compensates for
507 post-drought carbon loss in dry forests, *Nature Communications*, 10, 195, 2019.
- 508 Keyantash, J. and Dracup, J. A.: The quantification of drought: an evaluation of drought indices, *Bulletin of the American
509 Meteorological Society*, 83, 1167-1180, 2002.
- 510 Kumar, R., Musuuz, J. L., Loon, A. F. V., Teuling, A. J., Barthel, R., Ten Broek, J., Mai, J., Samaniego, L., and Attinger, S.:
511 Multiscale evaluation of the Standardized Precipitation Index as a groundwater drought indicator, *Hydrology and Earth System
512 Sciences*, 20, 1117-1131, 2016.



- 513 Lian, X., Piao, S., Huntingford, C., Li, Y., Zeng, Z., Wang, X., Ciais, P., McVicar, T. R., Peng, S., Ottlé, C., Yang, H., Yang, Y.,
514 Zhang, Y., and Wang, T.: Partitioning global land evapotranspiration using CMIP5 models constrained by observations, *Nature*
515 *Climate Change*, 8, 640-646, 2018.
- 516 Lloyd-Hughes, B.: The impracticality of a universal drought definition, *Theoretical and Applied Climatology*, 117, 607-611, 2014.
- 517 Maidment, R. I., Allan, R. P., and Black, E.: Recent observed and simulated changes in precipitation over Africa, *Geophysical*
518 *Research Letters*, 42, 8155-8164, 2015.
- 519 Mann, M. E. and Gleick, P. H.: Climate change and California drought in the 21st century, *Proceedings of the National Academy*
520 *of Sciences*, 112, 3858-3859, 2015.
- 521 Martens, B., Miralles, D. G., Lievens, H., van der Schalie, R., de Jeu, R. A., Fernández-Prieto, D., Beck, H. E., Dorigo, W. A., and
522 Verhoest, N. E.: GLEAM v3: satellite-based land evaporation and root-zone soil moisture, *Geoscientific Model Development*,
523 10, 1903, 2017.
- 524 Masih, I., Maskey, S., Mussá, F., and Trambauer, P.: A review of droughts on the African continent: a geospatial and long-term
525 perspective, *Hydrology and Earth System Sciences*, 18, 3635-3649, 2014.
- 526 McKee, T. B., Doesken, N. J., and Kleist, J.: The relationship of drought frequency and duration to time scales, 1993, 179-183.
- 527 Miralles, D. G., Holmes, T. R. H., De Jeu, R. A. M., Gash, J. H., Meesters, A. G. C. A., and Dolman, A. J.: Global land-surface
528 evaporation estimated from satellite-based observations, *Hydrol. Earth Syst. Sci.*, 15, 453-469, 2011.
- 529 Miralles, D. G., Van Den Berg, M. J., Gash, J. H., Parinussa, R. M., De Jeu, R. A., Beck, H. E., Holmes, T. R., Jiménez, C.,
530 Verhoest, N. E., and Dorigo, W. A.: El Niño–La Niña cycle and recent trends in continental evaporation, *Nature Climate*
531 *Change*, 4, 122, 2014.
- 532 Mishra, A. K. and Singh, V. P.: A review of drought concepts, *Journal of hydrology*, 391, 202-216, 2010.
- 533 Mo, K. C., Long, L. N., Xia, Y., Yang, S. K., Schemm, J. E., and Ek, M.: Drought Indices Based on the Climate Forecast System
534 Reanalysis and Ensemble NLDAS, *Journal of Hydrometeorology*, 12, 181-205, 2011.
- 535 Mu, Q., Zhao, M., Kimball, J. S., McDowell, N. G., and Running, S. W.: A remotely sensed global terrestrial drought severity
536 index, *Bulletin of the American Meteorological Society*, 94, 83-98, 2013.
- 537 Mukherjee, S., Mishra, A., and Trenberth, K. E.: Climate change and drought: a perspective on drought indices, *Current Climate*
538 *Change Reports*, 4, 145-163, 2018.
- 539 Muller, M.: Cape Town's drought: don't blame climate change. Nature Publishing Group, 2018.
- 540 Naumann, G., Alfieri, L., Wyser, K., Mentaschi, L., Betts, R. A., Carrao, H., Spinoni, J., Vogt, J., and Feyen, L.: Global Changes
541 in Drought Conditions Under Different Levels of Warming, *Geophysical Research Letters*, 45, 3285-3296, 2018.
- 542 Naumann, G., Dutra, E., Barbosa, P., Pappenberger, F., Wetterhall, F., and Vogt, J.: Comparison of drought indicators derived
543 from multiple data sets over Africa, *Hydrology and Earth System Sciences*, 18, 1625-1640, 2014.
- 544 Nemani, R. R., Keeling, C. D., Hashimoto, H., Jolly, W. M., Piper, S. C., Tucker, C. J., Myneni, R. B., and Running, S. W.:
545 Climate-Driven Increases in Global Terrestrial Net Primary Production from 1982 to 1999, *Science*, 300, 1560-1563, 2003.
- 546 Nicholson, S. E.: A detailed look at the recent drought situation in the Greater Horn of Africa, *Journal of Arid Environments*, 103,
547 71-79, 2014.
- 548 Panu, U. and Sharma, T.: Challenges in drought research: some perspectives and future directions, *Hydrological Sciences Journal*,
549 47, S19-S30, 2002.
- 550 Peña-Gallardo, M., Vicente-Serrano, S., Camarero, J., Gazol, A., Sánchez-Salguero, R., Domínguez-Castro, F., El Kenawy, A.,
551 Beguería-Portugués, S., Gutiérrez, E., and de Luis, M.: Drought Sensitiveness on Forest Growth in Peninsular Spain and the
552 Balearic Islands, *Forests*, 9, 524, 2018a.
- 553 Peña-Gallardo, M., Vicente-Serrano, S. M., Domínguez-Castro, F., Quiring, S., Svoboda, M., Beguería, S., and Hannaford, J.:
554 Effectiveness of drought indices in identifying impacts on major crops across the USA, *Climate Research*, 75, 221-240, 2018b.
- 555 Peng, J., Dadson, S., Hirpa, F., Dyer, E., Lees, T., Miralles, D. G., Vicente-Serrano, S. M. V.-S., and Funk, C.: High resolution
556 Standardized Precipitation Evapotranspiration Index (SPEI) dataset for Africa, Centre for Environmental Data Analysis, doi:
557 10.5285/bbdfd09a04304158b366777eba0d2aeb. , 2019a.
- 558 Peng, J., Dadson, S., Leng, G., Duan, Z., Jagdhuber, T., Guo, W., and Ludwig, R.: The impact of the Madden-Julian Oscillation on
559 hydrological extremes, *Journal of Hydrology*, 571, 142-149, 2019b.
- 560 Pinzon, J. E. and Tucker, C. J.: A non-stationary 1981–2012 AVHRR NDVI3g time series, *Remote Sensing*, 6, 6929-6960, 2014.
- 561 Richard, W., Sonia, I. S., Martin, H., Jinfeng, C., Philippe, C., Delphine, D., Joshua, E., Christian, F., Simon, N. G., Lukas, G.,
562 Alexandra-Jane, H., Thomas, H., Akihiko, I., Nikolay, K., Hyungjun, K., Guoyong, L., Junguo, L., Xingcai, L., Yoshimitsu,
563 M., Catherine, M., Christoph, M., Hannes Müller, S., Kazuya, N., Rene, O., Yadu, P., Thomas, A. M. P., Yusuke, S., Sibyll, S.,
564 Erwin, S., Justin, S., Tobias, S., Joerg, S., QiuHong, T., Wim, T., Yoshihide, W., Xuhui, W., Graham, P. W., Hong, Y., and
565 Tian, Z.: Evapotranspiration simulations in ISIMIP2a—Evaluation of spatio-temporal characteristics with a comprehensive
566 ensemble of independent datasets, *Environmental Research Letters*, 13, 075001, 2018.
- 567 Rivera, J. A., Marianetti, G., and Hinrichs, S.: Validation of CHIRPS precipitation dataset along the Central Andes of Argentina,
568 *Atmospheric Research*, 213, 437-449, 2018.
- 569 Schneider, U., Ziese, M., Meyer-Christoffer, A., Finger, P., Rustemeier, E., and Becker, A.: The new portfolio of global
570 precipitation data products of the Global Precipitation Climatology Centre suitable to assess and quantify the global water
571 cycle and resources, *Proceedings of the International Association of Hydrological Sciences*, 374, 29-34, 2016.



- 572 Schwalm, C. R., Anderegg, W. R. L., Michalak, A. M., Fisher, J. B., Biondi, F., Koch, G., Litvak, M., Ogle, K., Shaw, J. D., Wolf,
573 A., Huntzinger, D. N., Schaefer, K., Cook, R., Wei, Y., Fang, Y., Hayes, D., Huang, M., Jain, A., and Tian, H.: Global patterns
574 of drought recovery, *Nature*, 548, 202, 2017.
- 575 Sheffield, J., Wood, E. F., Chaney, N., Guan, K., Sadri, S., Yuan, X., Olang, L., Amani, A., Ali, A., and Demuth, S.: A drought
576 monitoring and forecasting system for sub-Saharan African water resources and food security, *Bulletin of the American*
577 *Meteorological Society*, 95, 861-882, 2014.
- 578 Shukla, S., McNally, A., Husak, G., and Funk, C.: A seasonal agricultural drought forecast system for food-insecure regions of
579 East Africa, *Hydrology and Earth System Sciences*, 18, 3907-3921, 2014.
- 580 Spinoni, J., Naumann, G., Vogt, J. V., and Barbosa, P.: The biggest drought events in Europe from 1950 to 2012, *Journal of*
581 *Hydrology: Regional Studies*, 3, 509-524, 2015.
- 582 Sun, Q., Miao, C., AghaKouchak, A., and Duan, Q.: Century-scale causal relationships between global dry/wet conditions and the
583 state of the Pacific and Atlantic Oceans, *Geophysical Research Letters*, 43, 6528-6537, 2016a.
- 584 Sun, S., Chen, H., Li, J., Wei, J., Wang, G., Sun, G., Hua, W., Zhou, S., and Deng, P.: Dependence of 3-month Standardized
585 Precipitation-Evapotranspiration Index dryness/wetness sensitivity on climatological precipitation over southwest China,
586 *International Journal of Climatology*, 38, 4568-4578, 2018.
- 587 Sun, S., Chen, H., Wang, G., Li, J., Mu, M., Yan, G., Xu, B., Huang, J., Wang, J., and Zhang, F.: Shift in potential
588 evapotranspiration and its implications for dryness/wetness over Southwest China, *Journal of Geophysical Research:*
589 *Atmospheres*, 121, 9342-9355, 2016c.
- 590 Swain, D. L., Tsiang, M., Haugen, M., Singh, D., Charland, A., Rajaratnam, B., and Diffenbaugh, N. S.: The extraordinary
591 California drought of 2013/2014: Character, context, and the role of climate change, *Bull. Am. Meteorol. Soc.*, 95, S3-S7,
592 2014.
- 593 Törnros, T. and Menzel, L.: Addressing drought conditions under current and future climates in the Jordan River region,
594 *Hydrology and Earth System Sciences*, 18, 305-318, 2014.
- 595 Toté, C., Patricio, D., Boogaard, H., van der Wijngaart, R., Tarnavsky, E., and Funk, C.: Evaluation of satellite rainfall estimates
596 for drought and flood monitoring in Mozambique, *Remote Sensing*, 7, 1758-1776, 2015.
- 597 Trambauer, P., Maskey, S., Winsemius, H., Werner, M., and Uhlenbrook, S.: A review of continental scale hydrological models
598 and their suitability for drought forecasting in (sub-Saharan) Africa, *Physics and Chemistry of the Earth, Parts A/B/C*, 66, 16-
599 26, 2013.
- 600 Um, M.-J., Kim, Y., Park, D., and Kim, J.: Effects of different reference periods on drought index (SPEI) estimations from 1901 to
601 2014, *Hydrology & Earth System Sciences*, 21, 2017.
- 602 van der Schrier, G., Barichivich, J., Briffa, K., and Jones, P.: A scPDSI-based global data set of dry and wet spells for 1901–2009,
603 *Journal of Geophysical Research: Atmospheres*, 118, 4025-4048, 2013.
- 604 van Dijk, A. I., Beck, H. E., Crosbie, R. S., de Jeu, R. A., Liu, Y. Y., Podger, G. M., Timbal, B., and Viney, N. R.: The
605 Millennium Drought in southeast Australia (2001–2009): Natural and human causes and implications for water resources,
606 ecosystems, economy, and society, *Water Resources Research*, 49, 1040-1057, 2013.
- 607 Van Loon, A. F.: *Hydrological drought explained*, Wiley Interdisciplinary Reviews: Water, 2, 359-392, 2015.
- 608 Vicente-Serrano, S.: Foreword: Drought complexity and assessment under climate change conditions, *Cuadernos de Investigación*
609 *Geográfica*, 42, 7-11, 2016.
- 610 Vicente-Serrano, S. M.: Evaluating the impact of drought using remote sensing in a Mediterranean, semi-arid region, *Natural*
611 *Hazards*, 40, 173-208, 2007.
- 612 Vicente-Serrano, S. M. and Beguería, S.: Comment on ‘Candidate distributions for climatological drought indices (SPI and SPEI)’
613 by James H. Stagge et al, *International Journal of Climatology*, 36, 2120-2131, 2016.
- 614 Vicente-Serrano, S. M., Beguería, S., Gimeno, L., Eklundh, L., Giuliani, G., Weston, D., El Kenawy, A., López-Moreno, J. I.,
615 Nieto, R., and Ayenew, T.: Challenges for drought mitigation in Africa: The potential use of geospatial data and drought
616 information systems, *Applied Geography*, 34, 471-486, 2012a.
- 617 Vicente-Serrano, S. M., Beguería, S., and López-Moreno, J. I.: A multiscalar drought index sensitive to global warming: the
618 standardized precipitation evapotranspiration index, *Journal of climate*, 23, 1696-1718, 2010.
- 619 Vicente-Serrano, S. M., Beguería, S., Lorenzo-Lacruz, J., Camarero, J. J., López-Moreno, J. I., Azorin-Molina, C., Revuelto, J.,
620 Morán-Tejeda, E., and Sanchez-Lorenzo, A.: Performance of Drought Indices for Ecological, Agricultural, and Hydrological
621 Applications, *Earth Interactions*, 16, 1-27, 2012b.
- 622 Vicente-Serrano, S. M., García-Herrera, R., Barriopedro, D., Azorin-Molina, C., López-Moreno, J. I., Martín-Hernández, N.,
623 Tomás-Burguera, M., Gimeno, L., and Nieto, R.: The Westerly Index as complementary indicator of the North Atlantic
624 oscillation in explaining drought variability across Europe, *Climate Dynamics*, 47, 845-863, 2016.
- 625 Vicente-Serrano, S. M., Gouveia, C., Camarero, J. J., Beguería, S., Trigo, R., López-Moreno, J. I., Azorin-Molina, C., Pasho, E.,
626 Lorenzo-Lacruz, J., Revuelto, J., Morán-Tejeda, E., and Sanchez-Lorenzo, A.: Response of vegetation to drought time-scales
627 across global land biomes, *Proceedings of the National Academy of Sciences*, 110, 52-57, 2013.
- 628 Vicente-Serrano, S. M., Miralles, D. G., Domínguez-Castro, F., Azorin-Molina, C., Kenawy, A. E., McVicar, T. R., Tomás-
629 Burguera, M., Beguería, S., Maneta, M., and Peña-Gallardo, M.: Global Assessment of the Standardized Evapotranspiration
630 Deficit Index (SEDI) for Drought Analysis and Monitoring, *Journal of Climate*, 31, 5371-5393, 2018.



- 631 Vicente-Serrano, S. M., Tomas-Burguera, M., Beguería, S., Reig, F., Latorre, B., Peña-Gallardo, M., Luna, M. Y., Morata, A., and
632 González-Hidalgo, J. C.: A high resolution dataset of drought indices for Spain, *Data*, 2, 22, 2017.
- 633 von Hardenberg, J., Meron, E., Shachak, M., and Zarmi, Y.: Diversity of vegetation patterns and desertification, *Physical Review*
634 *Letters*, 87, 198101, 2001.
- 635 Wang, H. and He, S.: The North China/Northeastern Asia Severe Summer Drought in 2014, *Journal of Climate*, 28, 6667-6681,
636 2015.
- 637 Wegren, S. K.: Food security and Russia's 2010 drought, *Eurasian Geography and Economics*, 52, 140-156, 2011.
- 638 Wilhite, D. and Pulwarty, R.: Drought as Hazard: Understanding the Natural and Social Context. In: *Drought and Water Crises:*
639 *Integrating Science, Management, and Policy*, 2017.
- 640 Wilhite, D. A., Svoboda, M. D., and Hayes, M. J.: Understanding the complex impacts of drought: A key to enhancing drought
641 mitigation and preparedness, *Water resources management*, 21, 763-774, 2007.
- 642 Xu, Y., Wang, L., Ross, K. W., Liu, C., and Berry, K.: Standardized Soil Moisture Index for Drought Monitoring Based on Soil
643 Moisture Active Passive Observations and 36 Years of North American Land Data Assimilation System Data: A Case Study in
644 the Southeast United States, *Remote Sensing*, 10, 301, 2018.
- 645 Yuan, X., Wood, E. F., Chaney, N. W., Sheffield, J., Kam, J., Liang, M., and Guan, K.: Probabilistic Seasonal Forecasting of
646 African Drought by Dynamical Models, *Journal of Hydrometeorology*, 14, 1706-1720, 2013.
- 647 Zambrano-Bigiarini, M., Nauditt, A., Birkel, C., Verbist, K., and Ribbe, L.: Temporal and spatial evaluation of satellite-based
648 rainfall estimates across the complex topographical and climatic gradients of Chile, *Hydrology and Earth System Sciences*, 21,
649 1295-1320, 2017.
- 650 Zhao, M., A, G., Velicogna, I., and Kimball, J. S.: A Global Gridded Dataset of GRACE Drought Severity Index for 2002–14:
651 Comparison with PDSI and SPEI and a Case Study of the Australia Millennium Drought, *Journal of Hydrometeorology*, 18,
652 2117-2129, 2017.
- 653 Zhou, Q., Leng, G., and Peng, J.: Recent Changes in the Occurrences and Damages of Floods and Droughts in the United States,
654 *Water*, 10, 1109, 2018.
- 655 Ziese, M., Schneider, U., Meyer-Christoffer, A., Schamm, K., Vido, J., Finger, P., Bissolli, P., Pietzsch, S., and Becker, A.: The
656 GPCC Drought Index—a new, combined and gridded global drought index, *Earth System Science Data*, 6, 285-295, 2014.

657

658